DEMONSTRATION OF COMMUNICATION USING NEUTRINOS

D.D. Stancil[1], P. Adamson[2], M. Alania[3], L. Aliaga[4], M. Andrews[2], C. Araujo Del Castillo[4],
L. Bagby[2], J.L. Bazo Alba[4], A. Bodek[5], D. Boehnlein[2], R. Bradford[5], W.K. Brooks[6], H. Budd[5],
A. Butkevich[7], D.A.M. Caicedo[8], D.P. Capista[2], C.M. Castromonte[8], A. Chamorro[3],
E. Charlton[9], M.E. Christy[10], J. Chvojka[5], P.D. Conrow[5], I. Danko[11], M. Day[5], J. Devan[9],
J.M. Downey[12], S.A. Dytman[11], B. Eberly[11], J.R. Fein[11], J. Felix[13], L. Fields[14],
G.A. Fiorentini[8], A.M. Gago[4], H. Gallagher[15], R. Gran[16], J. Grange[17], J. Griffin[5], T, Griffin[2],
E. Hahn[2], D.A. Harris[2], A. Higuera[13], J.A. Hobbs[14], C.M. Hoffman[5], B.L. Hughes[1],
K. Hurtado[3], A. Judd[5], T. Kafka[15], K. Kephart[2], J. Kilmer[2], M. Kordosky[9], S.A. Kulagin[7],
V.A. Kuznetsov[14], M. Lanari[16], T. Le[18], H. Lee[5], L. Loiacono[5,19], G. Maggi[6], E. Maher[20],
S.Manly[5], W.A. Mann[15], C.M. Marshall[5], K.S. McFarland[5,2], A. Mislivec[5], A. M. McGowan[5],
J.G. Morfín[2], H. da Motta[8], J. Mousseau[17], J.K. Nelson[9], J.A. Niemiec-Gielata[5], N. Ochoa[4],
B. Osmanov[17], J. Osta[2], J.L. Palomino[8], J.S. Paradis[5], V. Paolone[11], J. Park[5], C. Peña[6],
G. Perdue[5], C.E. Pérez Lara[4], A.M. Peterman[14], A. Pla-Dalmau[2], B. Pollock[9], F. Prokoshin[6],
R.D. Ransome[18], H. Ray[17], M. Reyhan[18], P. Rubinov[2], D. Ruggiero[5], O.S. Sands[12],
H. Schellman[14], D.W. Schmitz[2], E.C. Schulte[18], C. Simon[21], C.J. Solano Salinas[3], R. Stefanski[2],
R.G. Stevens[19], N. Tagg[22], V. Takhistov[18], B.G. Tice[18], R.N. Tilden[14], J.P. Velásquez[4],
I. Vergalosova[18], J. Voirin[2], J. Walding[9], B.J. Walker[14], T. Walton[10], J. Wolcott[5],
T.P. Wytock[14], G. Zavala[13], D. Zhang[9], L.Y. Zhu[10], and B.P. Ziemer[21]

[1] Department of Electrical and Computer Engineering, North Carolina State University, Raleigh, NC 27695,
[2] Fermi National Accelerator Laboratory, Batavia, IL 60510,
[3] Universidad Nacional de Ingenieria, Av. Tupac Amaru 210, Lima, Peru,
[4] Sección Física, Departamento de Ciencias, Pontificia Universidad Católica del Peru, Apartado 1761, Lima, Peru,
[5] Department of Physics and Astronomy, University of Rochester, Rochester NY 14627.
[6] Departamento de Física, Universidad Técnica Federico Santa María, Avda. España 1680 Casilla 110-V Valparaíso, Chile,
[7] Institute for Nuclear Research of the Russian Academy of Sciences, 117312 Moscow, Russia,
[8] Centro Brasileiro de Pesquisas Físicas, Rua Dr. Xavier Sigaud 150, Urca, Rio de Janeiro, RJ, 22290-180, Brazil,
[9] Department of Physics, College of William & Mary, Williamsburg, VA 23187,
[10] Hampton University, Dept. of Physics, Hampton, VA 23668,
[11] Department of Physics and Astronomy, University of Pittsburgh, Pittsburgh, PA 15260,
[12] NASA Glenn Research Center, Cleveland OH 44135,
[13] Departamento de Física, Universidad de Guanajuato, Campus León, Lomas del Bosque 103, fracc. Lomas del Campestre León GTO. 37150, México,
[14] Northwestern University, Evanston, IL 60208,
[15] Physics Department, Tufts University, Medford, MA 02155,
[16] Department of Physics, University of Minnesota - Duluth, Duluth, MN 55812,
[17] University of Florida, Department of Physics, Gainesville, FL 32611,
[18] Rutgers, The State University of New Jersey, Piscataway, NJ 08854,
[19] Department of Physics, University of Texas, 1 University Station, Austin, TX 78712.
[20] Massachusetts College of Liberal Arts, 375 Church St., North Adams, MA 01247,
[21] Department of Physics and Astronomy, University of California, Irvine, Irvine, CA 92697-4575,
[22] Otterbein College, One Otterbein College, Westerville, OH, 43081

ddstancil@ncsu.edu

Beams of neutrinos have been proposed as a vehicle for communications under unusual circumstances, such as direct point-to-point global communication, communication with submarines, secure communications and interstellar communication. We report on the performance of a low-rate communications link established using the NuMI beam line and the MINERvA detector at Fermilab. The link achieved a decoded data rate of 0.1 bits/sec with a bit error rate of 1% over a distance of 1.035 km, including 240 m of earth.

Keywords: Neutrino; Communication.

The use of fundamental particles that interact very weakly with matter has been proposed as a vehicle for communication in environments where electromagnetic waves are damped and do not penetrate easily. The bulk of these proposals have involved neutrinos,[1,2,3,4,5,6] although recent consideration has also been given to possible use of hypothetical particles such as the axion[7] and the hidden-sector photon.[8] Neutrino communication systems have been proposed for point-to-point global communications,[2] global communication with submarines,[2,6] and for interstellar communication.[3,4] Neutrino communication systems can also be contemplated for use in planetary exploration during periods in which the communications link is blocked by a planetary body. Even low bandwidth global point-to-point links could be useful for secure exchange of encryption codes. While the ability to penetrate matter is an important advantage of neutrinos, the weak interactions of neutrinos also imply that very intense beams and massive detectors would be required to realize this type of communication.

We report on the performance of a low-rate communications link established using the NuMI beam line and the MINERvA detector at Fermilab. The link achieved a decoded data rate of 0.1 bits/sec with a bit error rate of 1% over a distance of 1.035 km that included 240 m of earth. This demonstration illustrates the feasibility of using neutrino beams to provide a low-rate communications link, independent of any existing electromagnetic communications infrastructure. However, given the limited range, low data rate, and extreme technologies required to achieve this goal, significant improvements in neutrino beams and detectors are required for "practical" application.

The Neutrino beam at the Main Injector (NuMI)[9] at Fermilab is currently one of the most intense high energy neutrino beams worldwide, and provides a variable-energy beam for use in particle physics experiments. A simplified schematic of the beam line is shown in Fig. 1. A series of accelerators currently produces 8.1 μs pulses of 120 GeV protons every 2.2 s. The repetition rate is limited by the time required to accelerate the protons to high energy. The proton beam strikes a carbon target that produces many pions, kaons, and other particles. Charged particles are focused using magnets to produce a beam that is directed toward detectors. Almost all pions and kaons decay into neutrinos (mostly muon neutrinos and other associated particles) in a 675 m helium-filled decay pipe, in roughly the same direction as the momentum

of the original meson. This beam of assorted elementary particles passes through 240 meters of rock (mostly shale), and all particles are absorbed, except the neutrinos that define the NuMI beam. Since proton-carbon interactions at 120 GeV produce pions much more readily than kaons, the beam is predominantly composed of muon neutrinos (88%) with smaller components of muon antineutrinos (11%) and electron neutrinos (1%). The energy spectrum peaks at 3.2 GeV, and has a width (FWHM) of about 2.8 GeV. Although the energies extend to 80 GeV, 91.6% of the neutrinos in the beam have energies below 10 GeV. The detector is slightly more than 1 km from the target, and, at its peak energy, the beam has a transverse size of a few meters at the face of the detector.
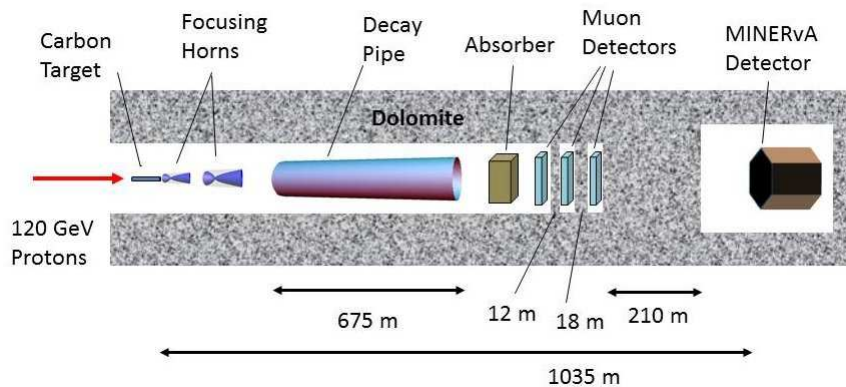

Fig. 1.   Layout of the NuMI beam line used as the neutrino source, and the MINERvA detector.

The MINERvA detector (Fig. 2) is located in a cavern about 100 m underground. Cross sections for neutrino interactions are measured by observing the trajectories of particles emitted when neutrinos interact with atomic nuclei in the material of the detector (carbon, lead, iron, water, helium and scintillator). The basic element of the detector is a hexagonal plane assembled from parallel triangular scintillating strips. The full detector has 200 such planes, and a total weight of 170 tons. The detector planes have one of three orientations rotated from each other by 60 degrees, and are labeled X, U, or V depending on the orientation. Analyses in the MINERvA experiment focus on neutrino interactions in the central tracker, comprising a three-ton detector that is fully sensitive to particles produced in the neutrino collisions. A charged particle passing through a scintillator produces scintillation light proportional to its deposited energy. When the light passes through wavelength shifting fibers embedded in the scintillator, fluorescent dopants in the fibers emit light at a new (green) wavelength, much of which is then transmitted through the optical fibers. Optical cables transport that light to photomultiplier tubes located above the detector. These signals are used to determine the deposited energy of the particle and the position of the particle in two dimensions. In turn, this information

4

is used to reconstruct particle identities and their trajectories in three dimensions by combining the X, U and V views to determine the products of the neutrino interaction. The central tracker is surrounded by calorimeters that have alternating layers of metal and scintillator used to contain high energy showering particles and measure their energy. The detector was designed to collect more than 16 million neutrino events over four years of beam time.
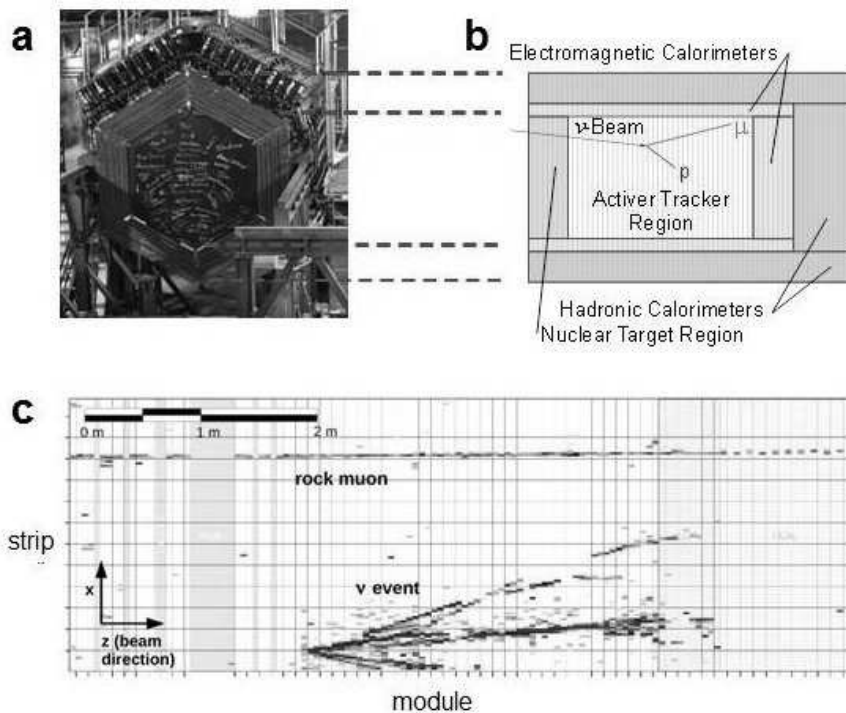

Fig. 2. The MINERvA detector. (a) Photograph. (b) Cross sectional diagram of the detector (c) Events in the detector from a single beam pulse that contains both kinds of events (neutrino interactions in the target and in the rock before the target) considered in this measurement. Each pixel contains position and energy information, and the display shows just the central region of the tracker (only the central portion was used).

The signal for this measurement is charged-current neutrino interactions that contain muons in the final state. The range of these muons is typically many meters in the plastic scintillator, so that each muon leaves a signal in at least several tens of scintillator strips, and such events are distinguished by their long and straight trajectories. The efficiency for reconstructing these long muon tracks is better than 95%, and there is a very small probability, negligible for the purposes of this demonstration, of finding such a muon candidate with the beam off.

In this demonstration, most of the signal is from neutrino interactions in the

rock upstream of MINERvA that produce muons that enter the upstream face of the detector. A smaller component of the signal is from neutrino interactions that produce muons in the active region of the detector. At the reduced intensity of 2.25×10^{13} protons per pulse used in this study of neutrino communication, an average of 0.81 events is registered during each pulse, through the use of a software filter to identify these two classes of signal muons that indicate the beam is "on". With a time resolution of a few nanoseconds for the muons selected for this demonstration of principle, it is possible to disentangle multiple events in the 8.1 μs beam bursts. An example of multiple events resulting from a single beam pulse is shown in Fig. 3. Figure 4 shows a histogram of the number of muons seen per beam pulse when the beam is not modulated. The close correspondence between data and a Poisson distribution shows the uncorrelated nature of our events, which is assumed in the statistical analysis of the communications experiment.
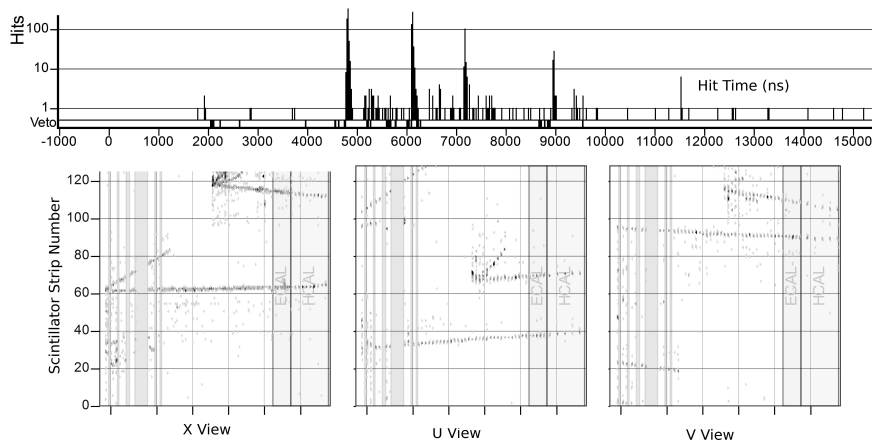

Fig. 3.   Example of track images from the MINERvA detector. The upper panel shows 6 separate events occurring at different times during an 8.1 μs neutrino pulse. The time measurements separate them easily. A superposition of tracks from these 6 events is shown for the X, U, and V planes as a function of module number in the stack in the lower panels. The horizontal axis is distance (about 3.6 cm/module) along the axis of the central tracker, and the vertical axis is distance (about 1.8 cm per strip) in directions perpendicular to the central axis.

The simplest method for encoding information about the neutrino beam is on-off keying (OOK). In this scheme, a "1" or a "0" is represented by the presence or absence of a beam pulse, respectively. In the NuMI beam line, OOK was implemented by controlling proton beam pulses from the Main Injector. Because the beam has a specific pulsed time structure, and because there are many independent detector segments, the chance of seeing an event that is not caused by the NuMI beam, e.g., from cosmic rays, is extremely small. A "1" bit corresponds to a beam pulse with an observed event or events, and a "0" bit is a pulse with no events.
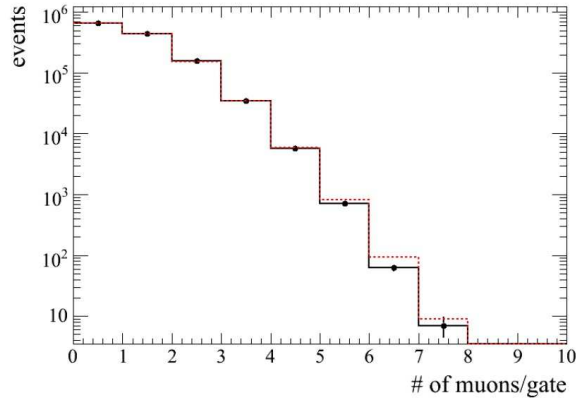
6

Fig. 4.   Muons per beam pulse in a run without beam modulation and higher beam intensity than available for this experiment. The black histogram is data and the dotted histogram is a Poisson distribution for the appropriate mean. The statistical error bars are in most cases smaller than the data points.

If the occurrence of events is modeled as a random Poisson process, this channel is mathematically equivalent to the photon counting (or Poisson) channel in communication theory[10] that models direct-detection of optical communications. In this model, the probability that no events are observed during a pulse is $e^{-\lambda}$, where λ is the expected number of events per pulse when the beam is "on". Since the neutrino detection system produces no errors when a 0 is sent, the probability of a bit error, or bit-error rate (BER), is $e^{-\lambda}/2$, assuming that 1 and 0 are equally likely.

The structure of the message is shown in Fig. 5a. The 8-character word "neutrino" is expressed in an abbreviated 5-bit code obtained by omitting the first two (left-most) bits in the standard 7-bit American Standard Code for Information Interchange (ASCII) code. This 40-bit message is subsequently encoded using the convolutional code with rate $\frac{1}{2}$ and constraint length 7, that is, in the NASA/ESA Planetary Standard,[11] and expands the message to 92 bits. This encoded message is concatenated with a 64-bit pseudo-noise (PN) synchronization sequence to form a 156-bit frame. This frame is repeated for the duration of the communication experiment. The accelerator throughout this study was operated at 25 pulses spaced by 2.2 s, followed by a 6.267 s interval to form a 61.267 s "supercycle."

The data received consists of 3454 records spanning an interval of just over 142 minutes, along with time stamps for each record. The detector is read out whenever a timing gate is received, independent of the presence of any beam. Each record contains the number of events observed in the detector over the duration of a beam pulse. Decoding the message requires the locations of the frames within the data. This is done by searching for the 64-bit PN sequence as a "sync" word that signals the end of each frame. If $x_0, \ldots, x_{N-1}$ is the entire sequence of transmitted bits and $K_0, \ldots, K_{N-1}$ the corresponding received counts, then K_i should be a
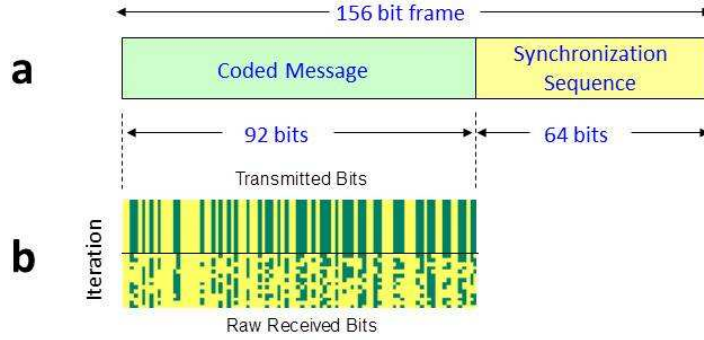
Fig. 5.   Format and representations of transmitted data. (a) Frame structure of the transmission. (b) Depictions of the transmitted and received data.

Poisson random variable with parameter $\lambda x_i + \lambda_0$, where λ is the expected number of events from a transmitted pulse, and $\lambda_0 \ll \lambda$ is the number of background events, which is nearly zero in this test. If the counts are conditionally independent, given $x_0, \ldots, x_{N-1}$, the receiver model is then mathematically equivalent to the direct-detection optical channel.[12] We searched for the end of a known sync word, e.g., $S_0, \ldots, S_{L-1}$, by finding the maxima of the log-likelihood statistic

$$\Lambda(m) = \sum_{j=0}^{L-1} \left(S_{L-1-j} - \frac{1}{2} \right) K_{m-j}. \tag{1}$$

However, to ensure symbol synchronization throughout the frame we search for two sync words spaced exactly by $m_0 = 156$ counts, so that the test statistic becomes $\Gamma(m) = \Lambda(m) + \Lambda(m - m_0)$. At the end of a sync word, this statistic has a mean $\mu = L\lambda/2$ and variance $\sigma^2 = L\lambda/2$. To detect a frame, we looked for m such that $\Gamma(m) \geq \mu - 2\sigma$. If half the bits are zero and $\lambda_0 \approx 0$, an estimate of λ is obtained by noting that 1402 events are observed in 3454 counts, so that $\lambda \approx 2 \times 1402/3454 = 0.81$. As illustrated in Fig. 6, this statistic identifies 15 frames with symbol synchronization, indicated by open circles. There are clearly other frames present that might be decoded successfully with more advanced processing; nevertheless, we will not pursue this here.

The 15 synchronized frames are used to recover the message and to estimate the properties of the channel. For any nonzero count, the bit is estimated to be 1, and 0 otherwise. Figure 5b illustrates message recovery in pictorial form, with each row of pixels in the top half of the image representing the transmitted data in one of the 15 frames, where dark pixels represent ones and light pixels are zeros. The bottom half of Fig. 5b shows the corresponding estimated bits at the receiver, where most (78%) are received correctly. Errors can be reduced by combining multiple frames and by using the convolutional error-control code. The optimal way to combine frames is to
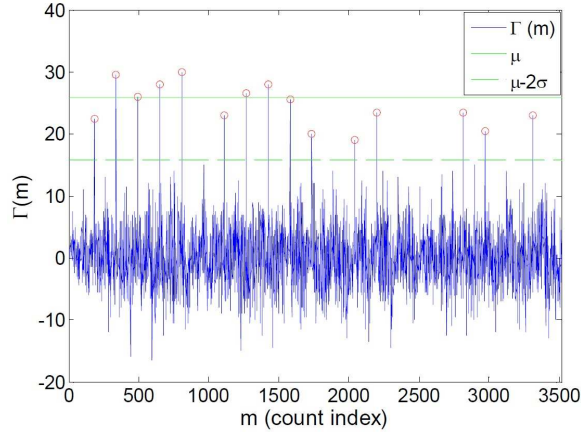
8

Fig. 6.   Statistic used for synchronization of frames. The open circles identify the locations of correctly reconstructed frames. Some frames were not correctly found because of accelerator aborts or data acquisition deadtimes.

add the corresponding event counts. In fact, the transmitted message is recovered perfectly if the results of all the frames are pooled, since events are observed in each column where a "1" is transmitted, and no events occur in any column where a "0" is transmitted. Consequently, this result demonstrates the ability to communicate information using neutrinos.

Figure 7 illustrates the relationship between the number of frames combined and the uncoded bit-error rate (BER) of the channel, which is the average fraction of incorrect received bits. Also shown for comparison is the theoretical uncoded BER of the Poisson prediction of BER $= e^{-\lambda}/2$ for $\lambda = 0.81$. The measured results are in close agreement (within expected fluctuations) with the Poisson model. It should be noted that 99% of the transmitted bits are decoded correctly using only 5 frames. No errors were observed for any combination of 9 or more frames.

Figure 7 also shows the BER after error-control decoding with the Viterbi algorithm.[11] These values are in very good agreement with the simulated Poisson channel for $\lambda = 0.81$ for the same type of decoding. In this case, $\approx 99\%$ of the transmitted bits are received correctly after only two frames, and no decoding errors are observed when any three frames are combined.

The theoretical capacity of the photon counting channel with OOK modulation and background rate $\lambda_0 = 0$ is given by[13]

$$C/B = \log_2 \left[1 + (1 - e^{-\lambda}) \cdot \exp\left(-\frac{\lambda}{e^{\lambda} - 1} \right) \right] \quad \text{(bits/pulse)}, \tag{2}$$

where B is the pulse or baud rate (pulses/sec), C is the channel capacity (bits/s), and λ is the average number of events per pulse defined above. In our experiment $\lambda \approx 0.81$, which yields a theoretical capacity of $C/B \approx 0.37$ bits/pulse. For comparison, the message was decoded with a 1% error rate after two iterations, or for the
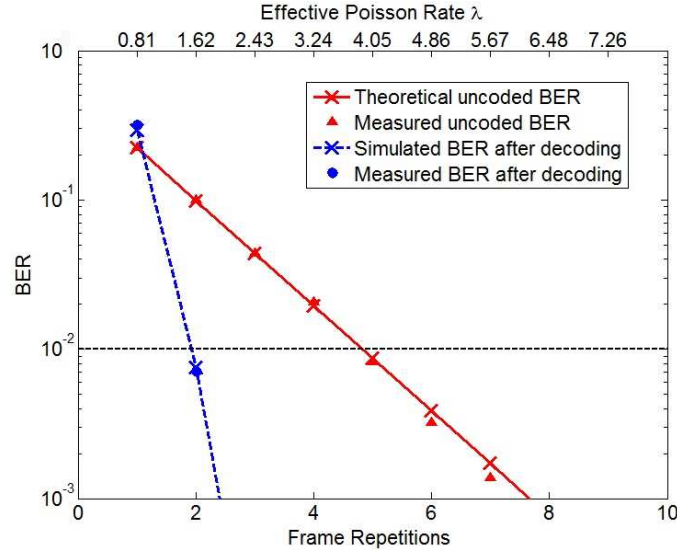
Fig. 7.   A comparison of predicted and measured bit-error rates, with and without error-control coding.

transmission of $2 \times 92 = 184$ pulses. Since there were only 40 bits of information transmitted, the experimental data rate can be estimated as 0.22 bits/pulse, or more than half the theoretical capacity of 0.37 bits/pulse. Since the pulse rate was about $1/2.2$ bits per second, the experimental data rate at an error probability of 1% can be estimated as $0.22 \times (1/2.2) \approx 0.1$ bits per second. We stress that this is only a rough estimate, since there are only 105 combinations of 2 frames selected from 15, and these combinations do not represent independent measurements because of reuse of the frames in forming the combinations.

In general, long-distance communication using neutrinos will favor detectors optimized for identifying interactions in a larger mass of target material than is visible to MINERvA and beams that are more intense and with higher energy neutrinos than NuMI because the beam becomes narrower and the neutrino interaction rate increases with neutrino energy. Of particular interest are the largest detectors, e.g., IceCube,[14] that uses the Antarctic icepack to detect events, along with muon storage rings to produce directed neutrino beams.[6,15]

In summary, we have used the Fermilab NuMI neutrino beam, together with the MINERvA detector to provide a demonstration of the possibility for digital communication using neutrinos. An overall data rate of about 0.1 Hz was realized, with an error rate of less than 1% for transmission of neutrinos through a few hundred meters of rock. This result illustrates the feasibility, but also shows the significant improvements in neutrino beams and detectors required for practical applications.

10

Acknowledgments

References

1. R. C. Arnold, *Science* **177**, 163 (1972).
2. A. W. Saenz, H. Uberall, F. J. Kelly, D. W. Padgett, N. Seeman, *Science* **198**, 295 (1977).
3. M. Subotowicz, *Acta Astronautica* **6**, 213 (1979).
4. J. G. Learned, S. Pakvasa, W. A. Simmons, X. Tata, *Quarterly Journal of the Royal Astro. Soc.* **35**, 321 (1994).
5. J. G. Learned, S. Pakvasa, A. Zee, *Phys. Lett. B* **671**, 15 (2009).
6. P. Huber, *Phys. Lett. B* **692**, 268 (2010).
7. D. D. Stancil, *Phys. Rev. D* **76**, 111701(R) (2007).
8. J. Jaeckel, J. Redondo, and A. Ringwald, *Europhys. Lett.* **87**, 10010 (2009).
9. K. Anderson, et al. *The NuMI Facility Technical Design Report.* FERMILAB-DESIGN-1998-01 (1998).
10. J. R. Pierce, E. C. Posner, and E. R. Rodemich, *IEEE Transactions on Information Theory* **IT-27**, 61 (1981).
11. D. J. Costello, Jr., et al. *IEEE Transactions on Information Theory* **IT-44**, 2531 (1998).
12. G. L. Liu, and H. H. Tan, *IEEE Transactions on Communications* **COM-24**, 227 (1986).
13. I. Bar-David and G. Kaplan, *IEEE Transactions on Information Theory* **IT-30**, 455 (1984).
14. F. Halzen and S. R. Klein, *Rev. Sci. Instrum.* **81** 081101-24 (2010).
15. S. Geer, *Phys. Rev. D* **57**, 6989 (1998).